Published for SISSA by Springer

Received: June 14, 2016
Revised: July 18, 2016
Accepted: August 11, 2016
Published: August 22, 2016

Unitarisation of EFT amplitudes for dark matter searches at the LHC

Nicole F. Bell,[a] **Giorgio Busoni,**[a] **Archil Kobakhidze,**[b] **David M. Long**[c] **and Michael A. Schmidt**[b]

[a] *ARC Centre of Excellence for Particle Physics at the Terascale, School of Physics, The University of Melbourne, Victoria 3010, Australia*

[b] *ARC Centre of Excellence for Particle Physics at the Terascale, School of Physics, The University of Sydney, NSW 2006, Australia*

[c] *School of Physics, The University of Sydney, NSW 2006, Australia*

E-mail: n.bell@unimelb.edu.au, giorgio.busoni@unimelb.edu.au, archil.kobakhidze@sydney.edu.au, dlon0938@uni.sydney.edu.au, michael.schmidt@sydney.edu.au

Abstract: We propose a new approach to the LHC dark matter search analysis within the effective field theory framework by utilising the K-matrix unitarisation formalism. This approach provides a reasonable estimate of the dark matter production cross section at high energies, and hence allows reliable bounds to be placed on the cut-off scale of relevant operators without running into the problem of perturbative unitarity violation. We exemplify this procedure for the effective operator D5 in monojet dark matter searches in the collinear approximation. We compare our bounds to those obtained using the truncation method and identify a parameter region where the unitarisation prescription leads to more stringent bounds.

Keywords: Beyond Standard Model, Effective field theories

ArXiv ePrint: 1606.02722

doi:10.1007/JHEP08(2016)125

JHEP08(2016)125

Contents

JHEP08(2016)125

1 Introduction

A dedicated search for Dark Matter (DM) at the Large Hadron Collider is currently one of the foremost objectives in particle physics. The most generic search channel is the mono-jet plus missing transverse energy signal, which searches for a single jet recoiling against the momentum of the DM particles which escape the detector unseen [1–6]. In order to make such a search possible, it is necessarily to have a framework in which to describe the interactions of dark matter particles with SM fields. Given the plethora of possible dark matter models in the literature, it is impractical to perform a dedicated analysis of each model. It is thus imperative to work with a small number of models that capture the essential aspects of the physics in some approximate way. Effective field theories (EFTs) achieve this aim, by parameterising the DM interactions with SM particles by a small set of non-renormalizable operators. For instance, the lowest order operators that describe the interaction of a pair of fermionic DM particles, χ, with a pair of SM fermions, f, are of the form

$$\frac{1}{\Lambda^2}\left(\overline{\chi}\Gamma_\chi\chi\right)\left(\overline{f}\Gamma_f f\right), \tag{1.1}$$

where the Lorentz structure $\Gamma_{\chi,f}$ can be $1, \gamma_5, \gamma_\mu, \gamma_5\gamma_\mu, \sigma_{\mu\nu}$. A full set of operators can be found in [7, 8], where a standard naming convention has been defined. Such operators are not intended to be complete description of DM interactions, valid at arbitrarily high energy. They would be obtained as a low energy approximation of some more complete theory by integrating out heavy degrees of freedom. The energy scale Λ is related to the parameters of that high energy theory as $\Lambda = g/M$, where g is a coupling constant and M is the mass of a heavy mediator.

The EFT description will clearly break down at energies comparable to Λ, at which scale we expect the mediators to be produced on-shell or give rise to cross section resonances. Moreover, while the EFT will provide physically well-behaved cross sections at low energies, they will give rise to bad high energy behaviour if used outside their region of validity. This manifests as a violation of perturbative unitarity [9–12]. While these issues may be remedied with a simplified model [13] in which a mediator is explicitly introduced, issues of unitarity violation can persist if gauge invariance is not respected. The shortcoming of EFTs and simplified models that violate SM gauge invariance [14–17] or dark-sector gauge invariance [18, 19] have recently been discussed.

Given the usefulness of the EFT and simplified model description of DM interactions, they will continue to be used in collider DM search analyses. Therefore, it is important to limit analyses to parameters that respect perturbative unitarity. One such approach is to use a truncation technique [20–22], which introduces a momentum cutoff equal to the mass of the would-be integrated-out mediator. In this paper we will instead use a procedure known as K-matrix unitarisation [23–28] to enforce unitarisation of all scattering amplitudes. Although this procedure will not capture the resonance structure of the true high energy theory, it will force scattering amplitudes to be well behaved at high energies, allowing us to derive meaningful limits on EFT models from LHC collisions with high centre of mass energies.

We will use the K-matrix approach to unitarise the 2 to 2 scattering amplitudes, such as $\overline{q}q \to \overline{\chi}\chi$. This will allow us to determine unitarised cross sections for the 2 to 3 mono-jet processes such as $\overline{q}q \to \overline{\chi}\chi g$, under the assumption that the gluon can be treated with the collinear approximation. We will also compare the results obtained from this unitarisation technique with those obtained with truncation. The rest of the paper is organised as follows: in section 2 we summarise the theoretical framework for the unitarisation procedure. We illustrate the unitarisation procedure in two toy models in section 3 and apply it to the standard vector operator D5 in section 4. Section 5 contains the conclusions, while in appendix A we derive the relevant cross sections in the collinear limit.

2 K-matrix unitarisation

The K-matrix formalism was first introduced in ref. [23, 24]. It is a technique to impose unitarity on amplitudes which naively violate unitarity. In the derivation we largely follow the notation and arguments in refs. [25, 26, 29].[1] Unitarity of the S-matrix,

$$S = \mathbb{I} + 2iT\,, \tag{2.1}$$

[1] See ref. [27, 28] for further details.

JHEP08(2016)125

implies the well-known relation for the T-matrix

$$T - T^\dagger = 2iTT^\dagger \,. \tag{2.2}$$

Note the factor of 2 in the definition of the T-matrix which has been introduced for convenience.

Following the seminal work by Jacob and Wick [27], for scattering processes $a\,b \to c\,d$ we can describe both the initial and the final state in terms of two-particle helicity states $|\Omega\lambda_1\lambda_2\rangle$ which are characterised by the helicities λ_i of the two particles and two angles θ and ϕ, collectively denoted Ω. Choosing the initial state to align with the z-axis, the individual T-matrix element for a process $a\,b \to c\,d$ with fixed helicities in the initial and final state is given by

$$\langle \Omega\lambda_c\lambda_d|T|0\lambda_a\lambda_b\rangle = \frac{1}{4\pi}\sum_J (2J+1)\, T^J_{\lambda'\lambda}\mathcal{D}^{J*}_{\lambda\lambda'}(\phi,\theta,0)\,, \tag{2.3}$$

in terms of the partial waves

$$T^J_{\lambda'\lambda} \equiv \langle J\lambda_c\lambda_d|T|J\lambda_a\lambda_b\rangle = \int d\Omega\, \langle \Omega\lambda_c\lambda_d|T|0\lambda_a\lambda_b\rangle\, \mathcal{D}^J_{\lambda\lambda'}(\phi,\theta,0)\,, \tag{2.4}$$

the Wigner D-functions $\mathcal{D}^J_{\lambda\lambda'}$ with total angular momentum J, and the resultant helicity of the two-particle states $\lambda = \lambda_a - \lambda_b$ and $\lambda' = \lambda_c - \lambda_d$, where we used the normalisation of the Wigner D-functions in ref. [26]. Assuming that no three-particle states are kinematically accessible, an analogous unitarity relation holds for each partial wave $T^J_{\lambda\lambda'}$ separately,

$$T^J - T^{J\dagger} = 2iT^{J\dagger}T^J, \tag{2.5}$$

in terms of matrices T^J with components $T^J_{\lambda'\lambda}$. This condition can be rewritten in terms of

$$\left(K^J\right)^{-1} \equiv \left(T^J\right)^{-1} + i\mathbb{I} = \left(\left(T^J\right)^{-1} + i\,\mathbb{I}\right)^\dagger\,, \tag{2.6}$$

which motivates the definition of the K-matrix for the J$^{\text{th}}$ partial wave, K^J. The K-matrix is hermitean, $K^J = K^{J\dagger}$. If the S-matrix is invariant under time reversal, the K-matrix is symmetric and thus K^J and $\left(K^J\right)^{-1}$ are real. Hence $(K^J)^{-1}$ can be considered as the real part of $(T^J)^{-1}$ and the imaginary part of T^J is determined by the term $i\mathbb{I}$ in eq. (2.6). We can invert the relation in eq. (2.6) to obtain

$$T^J \equiv \frac{1}{(K^J)^{-1} - i\mathbb{I}}\,. \tag{2.7}$$

The matrix T^J is given by the stereographic projection of the K-matrix on the Argand circle as shown in figure 1. If perturbative unitarity is violated in any amplitude, it can be enforced by imposing reality on $(K^J)^{-1}$, i.e. replacing $(K^J)^{-1}$ by $\mathrm{Re}[(T^J)^{-1}]$, which leads to the unitarised T-matrix[2]

$$T^J_U \equiv \frac{1}{\mathrm{Re}\left[(T^J)^{-1}\right] - i\mathbb{I}}\,. \tag{2.8}$$

[2]Note that this prescription is not analytic at $T^J = 0$ [29]. K-matrix unitarisation does not enforce a consistent analytic structure [30]. In practice this is not important, because we are interested in studying monojet searches at the LHC where the amplitudes are large and $T^J \neq 0$.

JHEP08(2016)125

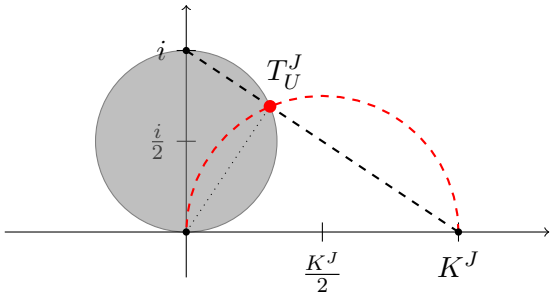

Figure 1. Argand circle and Thales projection.

Particularly in case the T-matrix quadratically grows with the centre of mass energy, $T^J \propto \frac{s}{16\pi\Lambda^2}$, the unitarised T-matrix asymptotically reaches saturation

$$T_U^J = \frac{1}{\frac{16\pi\Lambda^2}{s} - i} \overset{s\to\infty}{\longrightarrow} i\,, \tag{2.9}$$

which can be interpreted as a resonance at infinity. Note that the restriction to the real part of $\left(T^J\right)^{-1}$ can be understood as the Thales projection onto the real axis [29], if the T-matrix T^J is complex, i.e. points lying on the red dashed circle in figure 1 are projected onto the same unitarised T-matrix T_U^J as K^J. All discussed operators in sections 3 and 4 lead to a real T-matrix T^J in the considered scattering processes. Alternatively, following ref. [31, 32] the hermitean K-matrix can be considered as an approximation to the scattering amplitude, which can be obtained order by order in perturbation theory using eq. (2.6). Using the fact that the K-matrix is the Cayley transform of the S-matrix [33, 34]

$$S = \frac{\mathbb{I} + iK}{\mathbb{I} - iK}\,, \tag{2.10}$$

it is possible to reconstruct a unitary S-matrix starting from an approximate K-matrix. The S-matrix defined in eq. (2.10) restores unitarity, which is lost in the usual expansion of the S-matrix, if only a finite number of terms are taken into account in perturbation theory. The K-matrix formalism can be considered minimal, since it does not introduce new parameters or visible structures in scattering amplitudes like resonances. However it does not yield a viable UV completion of the effective theory. New resonances have to be included by hand. See refs. [29, 35, 36] for a recent discussion in the context of WW scattering.

In the following, we will make use of this prescription to obtain unitary amplitudes for DM pair production at the LHC. Taking the normalisation of the two-particle states properly into account, the T-matrix is related to the usual Lorentz-invariant matrix element $\mathcal{M}_{fi}$ by

$$\langle \Omega\lambda_c\lambda_d|T|0\lambda_a\lambda_b\rangle = \frac{1}{32\pi^2}\sqrt{\frac{4p_f p_i}{s}}\mathcal{M}_{fi}\,, \tag{2.11}$$

and analogously the partial waves. In the ultra-relativistic limit, the initial and final state phase space densities $2p_{i,f}/\sqrt{s}$ approach unity, simplifying the calculation of the unitarised

JHEP08(2016)125

T-matrix considerably. Finally, the differential cross section in terms of the T-matrix element is given by

$$\frac{d\sigma_{fi}}{d\Omega} = \frac{(4\pi)^2}{s}\frac{s}{4\,p_i^2}\left|\langle\Omega\lambda_c\lambda_d|T|0\lambda_a\lambda_b\rangle\right|^2 , \tag{2.12}$$

and thus the total cross section can be conveniently expressed in terms of the partial waves

$$\sigma_{fi} = \frac{4\pi}{s}\frac{s}{4\,p_i^2}\sum_J(2J+1)\left|T^J_{\lambda'\lambda}\right|^2 = \frac{4\pi}{s-4m_i^2}\sum_J(2J+1)\left|T^J_{\lambda'\lambda}\right|^2 . \tag{2.13}$$

Note that this is the cross section for fixed helicities. The unpolarised and color averaged cross section is obtained in the usual way by averaging over the initial state helicities and number of colours and summing over the final state ones, i.e.,

$$\sigma(q\bar{q}\to X) = \frac{1}{12}\sum_{\text{helicities}}\sigma_{fi} \tag{2.14}$$

for the unpolarised cross section $q\bar{q}\to X$ with two quarks in the initial state. The unitarised cross section is obtained by replacing $T^J_{\lambda'\lambda}$ by the corresponding unitarised T-matrix element $T^J_{U\lambda'\lambda}$. Thus the cross section is unitarised for each quark color and helicity separately.

3 Simple two-channel models

To illustrate the unitarisation procedure, we will make a simplifying assumption concerning the quark states in the operator and consider two simple models which feature only two channels. The effective operator D5 shall then be discussed in the next section.

3.1 States

As we are working in the collinear approximation, in the T-matrix we ought to consider all coupled two-particles states to expect the unitarity of the S-matrix to hold. If we consider the SM plus the DM particle coupled with an EFT operator, this implies the consideration of all possible two-particle states in the standard model with zero charge, baryon and lepton number, in addition to $\chi\bar{\chi}$. Taking into account color, helicity and flavour, this results in $3\cdot 3\cdot 4\cdot 6 = 216$ states for the quarks alone. To simplify the framework, we consider only the singlet color state

$$\frac{R\bar{R}+V\bar{V}+B\bar{B}}{\sqrt{3}} , \tag{3.1}$$

because all other color combinations decouple from this state and the DM sector. Moreover we assume the same operator suppression scale Λ for all quark flavours. In this case we can also consider just one flavour state:

$$\frac{u\bar{u}+d\bar{d}+s\bar{s}+c\bar{c}+b\bar{b}+t\bar{t}}{\sqrt{6}} , \tag{3.2}$$

as, again, all other flavour combinations decouple from this state and the DM sector. Now, if we "turn off" electro-weak interactions, i.e. approximating $\alpha_{EW}\ll\alpha_s$, this state decouples from all other standard model states, and only couples to itself and the DM states.

JHEP08(2016)125

3.2 EFT motivated by T-channel scalar exchange

We now consider a toy model scenario that can be solved analytically. We take the following EFT operator connecting the dark and the visible sector:

$$\mathcal{L}_1 = \frac{1}{\Lambda_{q\chi}^2}\bar{q}\gamma_\mu P_R q \bar{\chi}\gamma^\mu P_L \chi\,. \tag{3.3}$$

This operator can arise by integrating out a heavy coloured scalar t-channel mediator coupling only to right-handed quarks and left-handed DM particles. In the limit of massless particles, $s \gg m_\chi^2, m_q^2$, the only non-zero T-matrix elements are $\langle\chi_L\bar{\chi}_R|T|q_R\bar{q}_L\rangle$[3] and the matrix element $\langle q_R\bar{q}_L|T|\chi_L\bar{\chi}_R\rangle$ related by time-reversal. Thus we are left with a 2×2 T-matrix,

$$T = -\frac{1}{16\pi^2}\frac{s}{\Lambda_{q\chi}^2}\begin{pmatrix}0 & 1\\ 1 & 0\end{pmatrix}\sin^2\frac{\theta}{2}\,, \tag{3.4}$$

in the basis of the two helicity 1 two-particle states $(|q_R\bar{q}_L\rangle\,, |\chi_L\bar{\chi}_R\rangle)$. We only include the contribution of the effective operator and neglect any QCD contribution. The partial wave expansion only contains the term with total angular momentum $J = 1$,

$$T^1 = -\frac{1}{12\pi}\frac{s}{\Lambda_{q\chi}^2}\begin{pmatrix}0 & 1\\ 1 & 0\end{pmatrix}\,, \tag{3.5}$$

which grows linearly with s and thus is going to violate perturbative unitarity for scales $s \gtrsim 12\pi\Lambda_{q\chi^2}$. After unitarising the amplitudes using K-matrix unitarisation, the unitarised amplitude turns out to be

$$T_U^1 = \frac{1}{s^2 + 144\pi^2\Lambda_{q\chi}^4}\begin{pmatrix}is^2 & -12\pi s\Lambda_{q\chi}^2\\ -12\pi s\Lambda_{q\chi}^2 & is^2\end{pmatrix}\,. \tag{3.6}$$

Note that the unitarisation procedure introduces contributions to the scattering of $\bar{q}q \to \bar{q}q$ and $\bar{\chi}\chi \to \bar{\chi}\chi$. The denominator leads to a smooth cutoff around $s \sim 12\pi\Lambda_{q\chi}^2$, indicating that the non-unitarised amplitude strongly violates perturbative unitarity above such energy. When discussing the validity of the EFT, this in turn means that, unless new states and/or new interactions are introduced, the EFT breaks at this energy scale. The unitarised T-matrix is well-behaved for large s and converges to $i\mathbb{I}$ and it can be thus used to interpret scattering events, like monojet signatures at the LHC. In fact, the high-energy tail leads to a negligible contribution due to the suppression of the parton distribution function at high-energy in contrast to the EFT.

3.3 EFT motivated by S-channel vector boson exchange

Generally there might also be operators between two quark currents or two dark matter currents. As second example we consider an effective theory with three operators

$$\mathcal{L}_2 = \frac{1}{2\Lambda_{qq}^2}\bar{q}\gamma_\mu P_R q\bar{q}\gamma^\mu P_R q + \frac{1}{\Lambda_{q\chi}^2}\bar{q}\gamma_\mu P_R q\bar{\chi}\gamma^\mu P_R\chi + \frac{1}{2\Lambda_{\chi\chi}^2}\bar{\chi}\gamma_\mu P_R\chi\bar{\chi}\gamma^\mu P_R\chi\,, \tag{3.7}$$

[3]Note that right-handed (left-handed) particles have helicity $+\frac{1}{2}$ $(-\frac{1}{2})$.

JHEP08(2016)125

which might arise from a simplified model with a Z' gauge boson coupling only to the right-handed quark and DM currents. In such a model the EFT parameters are related to those of the UV complete theory according to $\Lambda_{qq}^2 = M_{Z'}^2/g_q^2$, $\Lambda_{q\chi}^2 = M_{Z'}^2/(g_q g_\chi)$ and $\Lambda_{\chi\chi}^2 = M_{Z'}^2/g_\chi^2$, where $g_{q,\chi}$ are the couplings of the Z' to the quarks and the DM, and $M_{Z'}$ is the mediator mass. The effective operators lead to four non-vanishing entries in the T-matrix, $\langle q_R\bar{q}_L|T|q_R\bar{q}_L\rangle$, $\langle \chi_R\bar{\chi}_L|T|\chi_R\bar{\chi}_L\rangle$, $\langle \chi_R\bar{\chi}_L|T|q_R\bar{q}_L\rangle$, and $\langle q_R\bar{q}_L|T|\chi_R\bar{\chi}_L\rangle$, where the latter two are related by time-reversal. The T-matrix in the basis $(|q_R\bar{q}_L\rangle\,, |\chi_R\bar{\chi}_L\rangle)$ is then given by

$$T = -\frac{1}{16\pi^2}\begin{pmatrix} \frac{2s}{\Lambda_{qq}^2} & \frac{s}{\Lambda_{q\chi}^2} \\ \frac{s}{\Lambda_{q\chi}^2} & \frac{2s}{\Lambda_{\chi\chi}^2} \end{pmatrix} \cos^2\frac{\theta}{2}\,. \tag{3.8}$$

Gluon s-channel exchange between quark - anti-quark pairs leads to an additional contribution to the $\langle q_R\bar{q}_L|T|q_R\bar{q}_L\rangle$ element. It does not grow with s like the other contributions and thus can be neglected for large s, when perturbative unitarity becomes an issue. The only non-vanishing term in the partial wave expansion has total angular momentum $J = 1$ reading

$$T^1 = -\frac{1}{12\pi}\begin{pmatrix} \frac{2s}{\Lambda_{qq}^2} & \frac{s}{\Lambda_{q\chi}^2} \\ \frac{s}{\Lambda_{q\chi}^2} & \frac{2s}{\Lambda_{\chi\chi}^2} \end{pmatrix}\,. \tag{3.9}$$

The expression for the unitarised T-matrix turns out to be complicated. Assuming an underlying simplified model with a Z' mediator, the operator suppression scales are related via

$$\Lambda_{qq}\Lambda_{\chi\chi} = \Lambda_{q\chi}^2\,. \tag{3.10}$$

This motivates the definition of the ratio

$$r = \frac{\Lambda_{q\chi}}{\Lambda_{\chi\chi}} = \frac{\Lambda_{qq}}{\Lambda_{q\chi}}\,. \tag{3.11}$$

In terms of the ratio r, the unitarised T-matrix, T^1, is

$$T_{U,r}^1 = \frac{1}{r^2s^2 - 8i\pi\left(r^4+1\right)s\Lambda_{q\chi}^2 - 48\pi^2r^2\Lambda_{q\chi}^4}\begin{pmatrix} is^2r^2 + 8\pi s\Lambda_{q\chi}^2 & 4\pi r^2 s\Lambda_{q\chi}^2 \\ 4\pi r^2 s\Lambda_{q\chi}^2 & is^2r^2 + 8\pi s\Lambda_{q\chi}^2 \end{pmatrix}\,. \tag{3.12}$$

Note that one can always parameterize new physics using a complete set of EFT operators like the ones in eq. (3.7), thus this choice is not model dependent, if one chooses a complete basis. The only model-dependent hypothesis we are using comes from imposing the relation (3.10) based on the assumption that the chosen EFT operators comes from an integrated-out Z' mediator. Even though this choice is model dependent, we will keep this constraint to reduce the number of parameters of the model. In the following we will restrict ourselves to this relation for simplicity and study the impact of the unitarisation procedure on the cross section using the well-studied D5 operator and the corresponding four-fermion operators with only quark and dark matter fields, respectively.

JHEP08(2016)125

4 Unitarising the effective operator D5

The K-matrix unitarisation procedure can be applied to any of the studied operators. We will focus on the operator D5[4] which might arise from a simplified model with a Z' gauge boson coupling to both the quark and DM vector currents. Besides the operator D5, whose Wilson coefficient we denote by $\Lambda_{q\chi}^{-2}$, we have to consider the two four-fermion operators with only quarks and DM particles χ, respectively

$$\mathcal{L}_{D5} = \frac{1}{2\Lambda_{qq}^2}\bar{q}\gamma_\mu q\bar{q}\gamma^\mu q + \frac{1}{\Lambda_{q\chi}^2}\bar{q}\gamma_\mu q\bar{\chi}\gamma^\mu\chi + \frac{1}{2\Lambda_{\chi\chi}^2}\bar{\chi}\gamma_\mu\chi\bar{\chi}\gamma^\mu\chi\,. \tag{4.1}$$

The explicit expressions for the T-matrix, the partial waves and the unitarised partial waves are summarised in appendix C. Similarly to the second toy model in the previous section, we assume relation (3.10) for simplicity and express the results in terms of the ratio (3.11). K-matrix unitarisation does not depend on this assumption, but it considerably simplifies the analysis by constraining the parameter space of the three Wilson coefficients to the two-dimensional submanifold defined by eq. (3.10).

Before comparing the result of K-matrix unitarisation with the 8 TeV ATLAS EFT limits for the operator D5 [3] and the method of truncation, we comment on the validity of the collinear approximation and the importance of quark jets.

4.1 Validity of collinear approximation

The collinear approximation is technically only valid in the limit of small scattering angles, i.e. small transverse momentum p_T compared to the centre of mass energy $\sqrt{s}$. Thus it is essential to estimate how well the collinear approximation performs for monojet searches, which usually employ a high cut on p_T to suppress QCD background. The full three-body final state cross section for the effective operator D5 with an emission of one gluon jet is presented in the appendix of ref. [21]. Figure 2 depicts the ratio of the cross section using the analytic result in ref. [21] over the cross section obtained in the collinear approximation as a function of the minimum $p_{T,\text{min}}$ both for 8 TeV (red line) and 13 TeV (blue line).[5] The collinear approximation leads to an enhancement of less than about 10% of the cross section for a minimum $p_{T,\text{min}} \simeq 100\,\text{GeV}$, which grows to 45% (30%) with $p_{T,\text{min}} = 800\,\text{GeV}$ for 8 TeV (13 TeV) centre of mass energy. The ATLAS 8 TeV monojet analysis [3] required $p_T > 120\,\text{GeV}$ and thus the collinear approximation overestimates the cross section by about 13%. The 13 TeV monojet searches plan to require $p_{T,\text{min}} = 600\,\text{GeV}$ leading to about 37% overestimation of the cross section by taking the collinear limit. We expect similar results for the cross section in the unitarised EFT, which is suggested by the fact that the cross section in the effective theory can be factorised in the two-body cross section $q\bar{q} \to \chi\bar{\chi}$ and a function dependent on the scattering angle of the jet and its rapidity. Consequently we expect the overestimation by taking the collinear limit to mostly cancel out in the ratio

[4] The operator D5 belongs to the list of operators presented in ref. [7], which have been widely used in the LHC monojet searches reported by the ATLAS and CMS collaborations. See table 1 for the full list of operators.

[5] Note that the collinear limit for the effective operators D1 and D4 agrees with the exact result.

JHEP08(2016)125

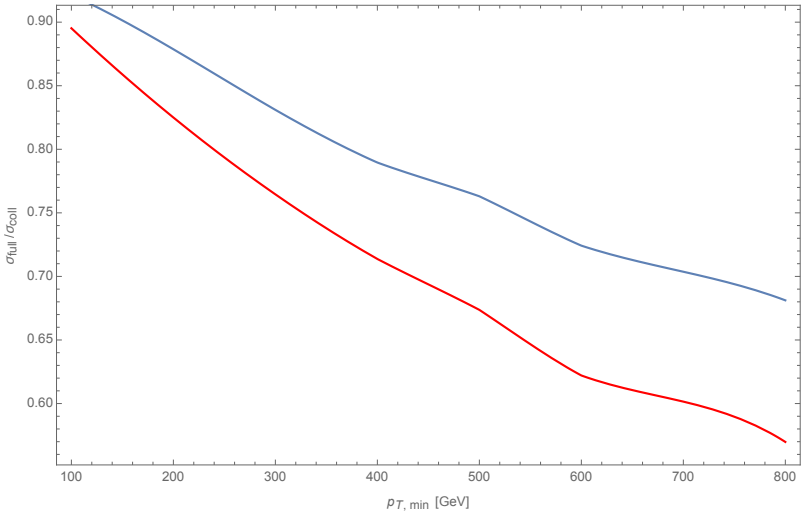

Figure 2. Ratio of the full cross section to the collinear one as a function of the minimum transverse momentum p_T for $m_{DM} = 100\,\text{GeV}$. The Blue line refers to beam energy of 13TeV, the red one to 8 TeV.

of the cross sections (R_U and R_Λ, defined below). Hence the ratios calculated with the collinear approximation will be closer to the values obtained from a full 3-body final state calculation than the result in figure 2 suggests. Thus the collinear approximation works well, which is also supported by a similar analysis in ref. [37]. Going beyond the collinear limit requires the inclusion of three-body states in the T-matrix rendering the K-matrix unitarisation procedure more complicated. We will defer an analysis beyond the collinear limit to a future publication.

4.2 Importance of quark-jets

In the previous subsection we only considered gluon jets, shown in figure 4a, and neglected the additional contribution from quark jets. It originates from diagrams with gluons in the initial state as shown in figure 4b. Quark jets generally lead to a 10% increase in the cross section, as it is suggested by figure 6 in ref. [21]. We included quark jets and show in figure 3 the ratio of the unitarised cross section over the cross section using the effective field theory in the collinear limit for a fixed value of the DM mass, $m_{DM} = 100\,\text{GeV}$,

$$R_U = \frac{\sigma_{\text{unitarised,coll.}}}{\sigma_{\text{EFT,coll.}}}\,, \tag{4.2}$$

for different values of $r = 1, 2, 5$. The dotted lines show the ratio R_U, if quark jets are neglected, while the solid lines take both contributions into account. The additional contribution of quark jets generally enhances the unitarised cross section over the EFT cross section.

4.3 Reinterpretation of the 8 TeV ATLAS monojet limit

ATLAS performed a monojet analysis with their full 8 TeV dataset of 20.3 fb^{-1}. The limits were interpreted for different EFT models including the operator D5. Besides the

JHEP08(2016)125

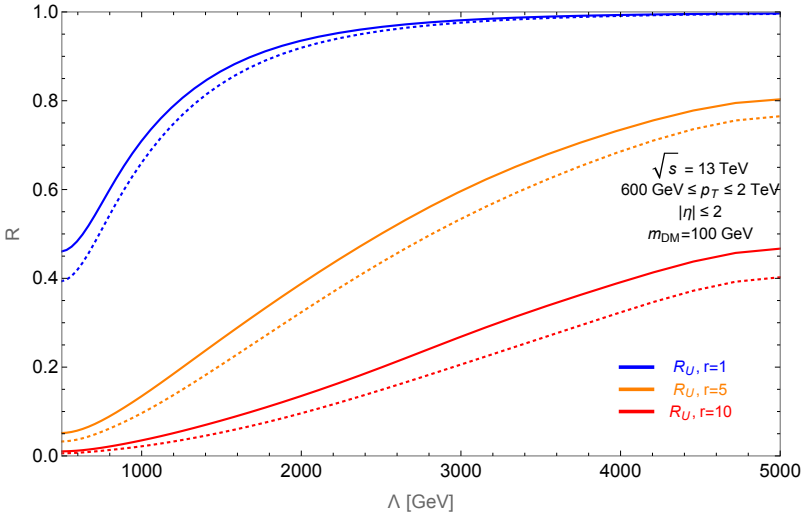

Figure 3. The ratio R_U as a function of the cut-off scale Λ, for different values of r for $m_{DM} = 100\,\text{GeV}$. The solid lines refer to R_U including both quark and gluon jets, the dotted lines refer to R_U including only gluon jets.

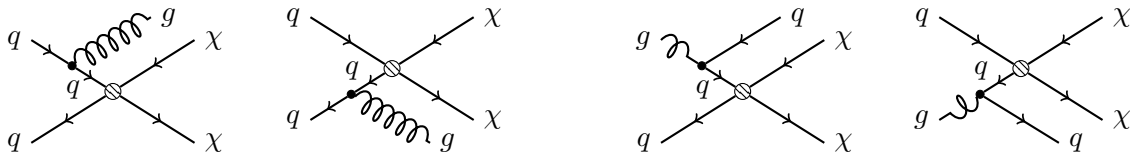

(a) Gluon jets. **(b)** Quark jets.

Figure 4. Initial state radiation leading to monojet signature in DM pair production at the LHC.

EFT limit, ATLAS also quotes the limit obtained using truncation, where only events are kept, which are consistent with the EFT interpretation and satisfy the constraint

$$\Lambda > \frac{Q_{tr}}{\sqrt{g_q g_\chi}} > 2\frac{m_{\text{DM}}}{\sqrt{g_q g_\chi}}\,, \tag{4.3}$$

i.e. the requirement that the momentum transfer Q_{tr} is always smaller than the mass of the mediator $M = \sqrt{g_q g_\chi}\Lambda$, which is expressed in terms of the cutoff scale Λ and the couplings $g_{q,\chi}$ of the quarks and DM particles χ to the mediator. In case of D5, this could be the mass of an Z' gauge boson, which is exchanged in the s-channel, and the corresponding gauge couplings with quarks and DM. For gauge couplings, we naively expect the couplings to be of a similar order of magnitude. We reproduce in figure 5 the official ATLAS 8 TeV monojet limit shown in figure 10b of ref. [3]. The blue solid line refers to the ATLAS EFT limit, and the green and yellow regions indicate the 1 and 2σ uncertainty bands. The red dashed line corresponds to the limit using truncation with maximal couplings $g_q g_\chi = 4\pi$ and the purple dashed line to the one using truncation with couplings $g_q g_\chi = 1$. The purple dotted line is our result for truncation with unit couplings using the collinear limit. The black solid lines show the limit obtained using the unitarised amplitude with $r = 1, 2, 3, 4, 5$ from top to bottom. The limits are only shown for small DM masses $m_{DM} < 100\,\text{GeV}$,

JHEP08(2016)125

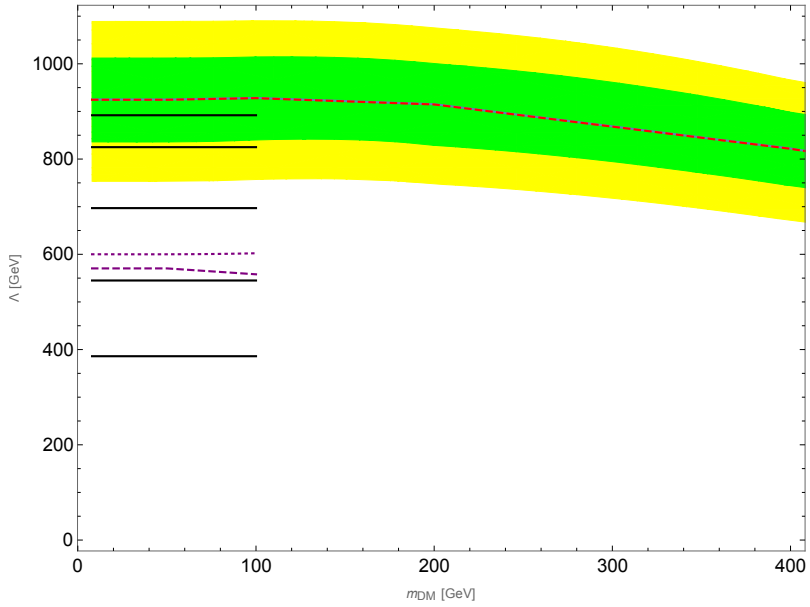

Figure 5. Reinterpretation of ATLAS limit at 8TeV. The blue line refers to the ATLAS limit, the green and yellow band indicating the 1 and 2 sigma uncertainty bands, as in [3]. The red dashed line indicates the limit using truncation with maximal couplings, the purple dashed one using truncation with unit couplings. The purple dotted lines refers to our result using the collinear limit for the truncation with unit couplings, while the black lines refer to the unitarised amplitude with $r = 1, 2, 3, 4, 5$ from top to bottom.

because they are derived neglecting the DM mass. In our analysis, we employ the collinear limit and only include the leading jet unlike the ATLAS analysis, which included a second jet. These effects go in the opposite direction and partly cancel each other. The unitarised amplitude with $r \leq 3$ leads to a stronger limit than using truncation with $g_q g_\chi = 1$.

4.4 Future projection to 13 TeV and comparison to truncation

Using the cross section ratio, it is straightforward to apply the same method to a future analysis. The EFT cross section is suppressed by the fourth power of the scale of the effective operator $\Lambda \equiv \Lambda_{q\chi}$. Thus a reduction of the unitarised cross section by a factor R_U approximately results in a decrease of the limit on the scale Λ by a factor of $R_U^{1/4}$. In practice the unitarised limit has to be obtained iteratively [38]. Figure 6 shows the ratio R_U as a function of the cutoff scale Λ for different values of $r = 1, 5, 10$ as solid lines. The dashed lines serve as a comparison to the corresponding ratio

$$R_\Lambda = \frac{\sigma_{\text{truncated,coll.}}}{\sigma_{\text{EFT,coll.}}}\,, \tag{4.4}$$

using the truncated amplitudes for different benchmark values of the couplings $g_q g_\chi = 0.5, 1, 2, 4\pi$. All ratios have been obtained using the collinear approximation including exactly one jet, which can be either a quark or a gluon jet. The centre of mass energy is fixed to $\sqrt{s} = 13\text{TeV}$ and the DM mass to $m_{DM} = 100\,\text{GeV}$. The transverse momentum

JHEP08(2016)125

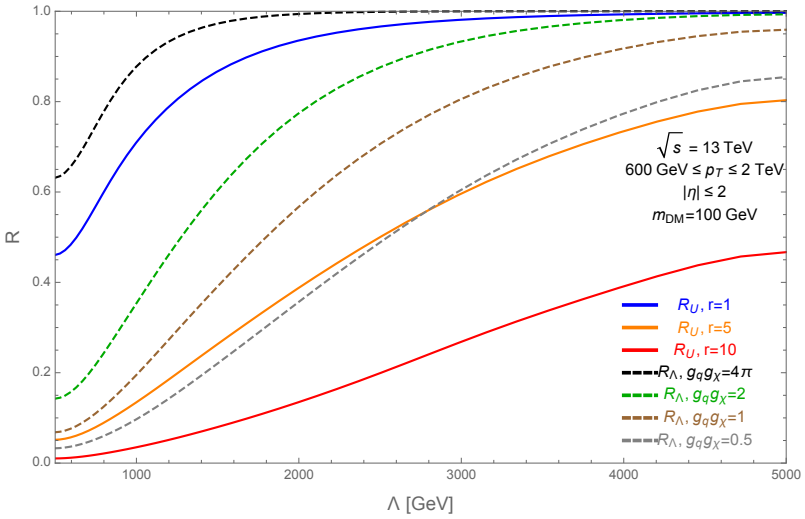

Figure 6. Quantities R_U, R_Λ as a function of the cut-off scale Λ for different values of $r = 1, 5, 10$ and $g_q g_\chi = 0.5, 1, 2, 4\pi$ for $m_{DM} = 100\,\text{GeV}$. The solid lines refer to R_U, the dashed lines refer to R_Λ. Both gluon and quark jets were included in both cases.

p_T is limited to $600\,\text{GeV} \leq p_T \leq 2\text{TeV}$ and rapidity is required to satisfy $|\eta| \leq 2$. The ratios R_U and R_Λ do not change much if the cut on p_T is slightly increased to 700 GeV.

The suppression is generally stronger for low cut-off scales Λ, because more events have to be discarded using the truncation procedure or the amplitude is reduced for smaller center of mass energies $\sqrt{s}$ using K-matrix unitarisation. The more a value deviates from $r = 1$, the more the unitarised cross section is suppressed, similar to smaller couplings $g_q g_\chi$ when using truncation. This can be clearly seen in figure 6.

The values of R_U reported in figure 6 can be used to rescale EFT limits in the same way as with R_Λ. The precise description of the rescaling procedure and its main consequences are outlined in ref. [38].

Finally we compare the K-matrix unitarisation to the truncation procedure in the figure 7. The solid lines show the lines of constant $g_q g_\chi = 0.5, 1, 8$ from left to right. The vertical dashed line indicates the current limit from dijet searches restricting $g_q \lesssim 0.25$ for mediator masses up to 3 TeV [39]. The light blue shaded region has $R_U < R_\Lambda$, i.e. unitarisation leads to a larger suppression of the cross section than truncation and thus a less stringent limit. Generally the truncated amplitude is less suppressed for $g_q g_\chi \gtrsim 3$ and thus leads to a stronger limit. In the region which is not excluded by the dijet constraint, i.e. $g_q \lesssim 0.25$, we find that the unitarisation method leads to a stronger limit, $R_U > R_\Lambda$, for $g_\chi \lesssim 1$.

5 Conclusions

Non-renormalisable operators lead to violation of perturbative unitarity in scattering amplitudes above the scale of the operator. This particularly poses a problem for the interpretation of monojet searches at the LHC experiments in terms of EFTs, because the limits on the cut-off scale Λ obtained assuming an EFT are lower than the centre of mass energy $\sqrt{s}$.

JHEP08(2016)125

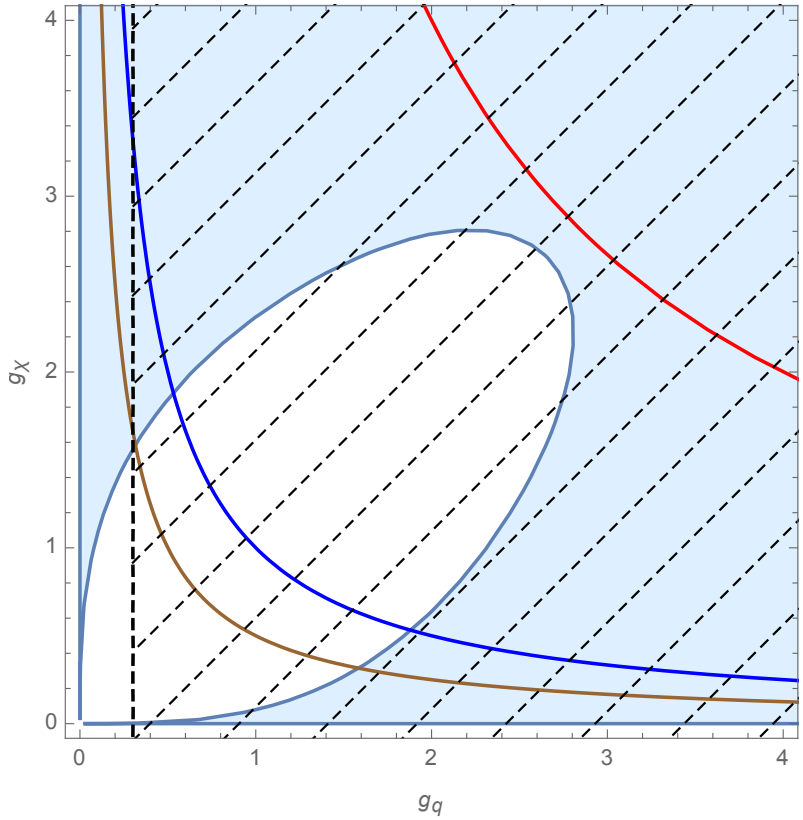

Figure 7. The light blue shaded region is the region of the parameter space with $R_U < R_\Lambda$. The region covered by black dashed lines is excluded by dijet search [39] (for mediators below 3TeV). The brown, blue and red lines are contours where the value of $g_q g_\chi$ is constant, and equal to 1/2 (brown), 1 (blue) and 8 (red).

Thus there are many high-energy collisions with a centre of mass energy greater than Λ. Although high-energy events are penalised by the small values of the parton distribution functions, this is cancelled by the enhanced scattering amplitude, which grows proportional to the centre of mass energy.

K-matrix unitarisation allows consistent limits to be obtained within the EFT framework. We exemplified this for the operator D5 as well as two other simple toy models. It leads to a smooth suppression of the scattering amplitude. In the limit of large centre of mass energy, $\sqrt{s} \to \infty$, the T-matrix approaches $i\mathbb{1}$ and thus the off-diagonal elements describing DM pair production at the LHC vanish. K-matrix unitarisation introduces a dependence on the other T-matrix elements and thus the cut-off scales of other operators, e.g. four quark operators and operators with four DM particles. The smallest cut-off scale among all relevant operators determines the scale when the suppression due to K-matrix unitarisation sets in. Hence the least suppression of the cross section in the K-matrix unitarisation framework is obtained if the cut-off scales are of a similar order of magnitude. This can be clearly seen for the D5 operator: the suppression increase with $r = \Lambda_{q\chi}/\Lambda_{\chi\chi}$, since the smallest cut-off scale decreases with r.

JHEP08(2016)125

We recast the ATLAS 8 TeV monojet limit on the operator D5 for five benchmark values of $r = 1, 2, 3, 4, 5$ finding a slight suppression of a few percent for $r = 1$ which grew to more than 50% for $r = 5$. Given the suppression of the cross section as a function of the cut-off scale Λ, it is straightforward to recast the limit obtained using an EFT to a limit for the unitarised EFT. We provide this ratio for three different choices of r, for a centre of mass energy of $\sqrt{s} = 13$TeV, which can be directly used to obtain the unitarised EFT limit given the EFT limit. Note however that all results have been obtained in the collinear approximation and without including a possible second jet. Going beyond these two approximations, and the application of the same procedure to the other considered operators, will be an interesting extension of the present work.

K-matrix unitarisation of EFT amplitudes provides a new way to extract model-independent and theoretically reliable limits on the dark matter production cross section at the LHC. The method can be applied to a wide class of scenarios, including other mono-X searches or simplified models without manifest gauge invariance, providing, in certain cases, more stringent limits than the truncation method currently used.

Acknowledgments

We thank Lei Wu for collaboration during the initial stages of this project. This work was supported in part by the Australian Research Council.

A Collinear approximation

The collinear approximation allows to drastically simplify the discussion. This appendix contains a detailed derivation of the relevant cross section. Starting by simplifying the three-body phase space, we can write

$$d\phi^{3\text{body}} = (2\pi)^4 \delta^4 \left(\sum_{i=1}^{3} p_i - p_0 \right) \prod_{i=1}^{3} \frac{d^3 p_i}{(2\pi)^3 2E_i} = \frac{1}{2^8 \pi^5} \frac{d^3 p_1 d^3 p_2}{E_1 E_2 E_3} \delta(E_1 + E_2 + E_3 - E_0) \,. \quad \text{(A.1)}$$

The phase space is Lorentz invariant, so we are free to evaluate this expression in any reference system. After introducing the four-momentum $p_{23} = p_2 + p_3$ with the corresponding energy $E_{23} = p_{23}^0$ and invariant four-momentum $s_{23} = p_{23}^2$, it is possible to use the identities

$$1 = ds_{23} \delta(s_{23} - p_{23}^2) \theta(p_{23}^0) \quad \text{(A.2)}$$

$$\delta(E_1 + E_2 + E_3 - E_0) = \delta(E_2 + E_3 - E_{23}) \delta(E_1 + E_{23} - E_0) dE_{23} \quad \text{(A.3)}$$

to separate the two-body phase space of particles 2 and 3

$$d\phi^{3\text{body}} = \frac{1}{2^8 \pi^5} \frac{d^3 p_1 d^3 p_2}{E_1 E_2 E_3} ds_{23} \delta(s_{23} - p_{23}^2) \theta(p_{23}^0) \delta(E_2 + E_3 - E_{23}) \delta(E_1 + E_{23} - E_0) dE_{23} \quad \text{(A.4)}$$

$$= \frac{1}{2^4 \pi^3} \frac{d^3 p_1}{E_1} ds_{23} \delta(s_{23} - p_{23}^2) \theta(p_{23}^0) \delta(E_1 + E_{23} - E_0) dE_{23} d\phi_{2,3}^{2\text{body}} \,, \quad \text{(A.5)}$$

where in the last step we have used the definition of the two-body phase space of the particles 2 and 3

$$d\phi_{2,3}^{\text{2body}} \equiv \frac{1}{2^4\pi^2}\frac{d^3p_2}{E_2E_3}\delta(E_2+E_3-E_{23})\,, \tag{A.6}$$

which will be included in the two-body cross section. The remaining part can be further simplified by integrating over E_{23}

$$d\phi^{\text{3body}} = d\phi_{2,3}^{\text{2body}}\frac{ds_{23}}{2\pi}\frac{1}{2^4\pi^2}\frac{d^3p_1}{E_1E_{23}}\delta(E_1+E_{23}-E_0)\,. \tag{A.7}$$

While we are not interested in simplifying $d\phi_{2,3}^{\text{2body}}$ further, as its expression in terms of kinematic variables will be necessary only to calculate the cross section $\sigma_{q\bar{q}\to\chi\bar{\chi}}$, we want to simplify the last delta function in

$$d\phi^{\text{3body}} = d\phi_{2,3}^{\text{2body}}\frac{ds_{23}}{2^4\pi^2}\frac{d\cos\theta_0 E_1 dE_1}{E_{23}}\delta(E_1+E_{23}-E_0)\,, \tag{A.8}$$

which can be evaluated using

$$E_{23} = \sqrt{E_1^2+s_{23}} \qquad\qquad \frac{dE_{23}}{dE_1} = \frac{E_1}{\sqrt{E_1^2+s_{23}}} = \frac{E_1}{E_{23}}\,. \tag{A.9}$$

Thus we obtain after the integration with respect to E_1

$$d\phi^{\text{3body}} = d\phi_{2,3}^{\text{2body}}\frac{ds_{23}d\cos\theta_0}{2^4\pi^2}\frac{E_1}{E_0} \tag{A.10}$$

The phase space and cross section are simple to evaluate in the centre of mass frame, where momentum fraction of the partons equal $x_1 = x_2 = x$ and the following kinematic relations hold

$$\hat{s} = (p_1+p_2+p_3)^2 = sx^2 \qquad\qquad E_1 = \sqrt{sx^2}\frac{z_0}{2} \tag{A.11}$$

$$s_{23} = (p_2+p_3)^2 = sx^2(1-z_0) \qquad\qquad E_{23} = \sqrt{sx^2}\left(1-\frac{z_0}{2}\right) \tag{A.12}$$

The definition of z_0, θ_0 is given in the following parametrisation of the momenta in the centre of mass frame

$$p_1^\mu = \sqrt{sx^2}\frac{z_0}{2}\,(1,0,\sin\theta_0,\cos\theta_0) \tag{A.13}$$

$$p_2^\mu = \sqrt{sx^2}\left(\frac{1-y_0}{2},\sqrt{(1-y_0)^2-a^2}\hat{p}_3\right) \tag{A.14}$$

$$p_3^\mu = \sqrt{sx^2}\left(\frac{1+y_0-z_0}{2},\sqrt{(1+y_0-z_0)^2-a^2}\hat{p}_4\right)\,, \tag{A.15}$$

where the angle between p_2 and p_1 is fixed by momentum conservation and the fraction $\frac{2m_{DM}}{\sqrt{sx^2}}$. Using this parametrisation allows us to write the three-body phase space as

$$d\phi^{\text{3body}} = d\phi_{2,3}^{\text{2body}}\frac{sx^2z_0}{32\pi^2}dz_0 d\cos\theta_0 \tag{A.16}$$

JHEP08(2016)125

clearly separating the two-body phase space factor from the variables z_0 and $\cos\theta_0$ describing the additional jet.

After the derivation of the convenient form of the three-body phase space factor, we are ready to work with the collinear approximation. The four-momentum of the jet is denoted p_1, while the four-momenta of the DM particles are $p_{2,3}$. Following the standard discussion of the collinear limit (See e.g. [40]), the monojet cross section with a gluon jet can be written as[6]

$$\begin{aligned} d\sigma_{q\bar{q}\to\chi\bar{\chi}+j(g)} &= \frac{1}{|v_q - v_{\bar{q}}|2E_q 2E_{\bar{q}}}\left[\frac{1}{2}\sum|M|^2\right]\frac{1}{(p_{q,\bar{q}}-p_1)^4}\frac{1}{4}\overline{|M|^2}_{q\bar{q}\to\chi\bar{\chi}}(s_{23})d\phi^{3\text{body}} \\ &= \frac{1}{2sx^2}\left[\frac{2g_s^2p_T^2}{z_0(1-z_0)}\frac{1+(1-z_0)^2}{z_0}\right]\frac{z_0^2}{p_T^4}\frac{1}{4}\overline{|M|^2}_{q\bar{q}\to\chi\bar{\chi}}(s_{23})d\phi_{2,3}^{2\text{body}}\frac{sx^2z_0}{32\pi^2}dz_0 d\cos\theta_0 \end{aligned} \tag{A.17}$$

neglecting the color factor. The four-momentum $p_{q,\bar{q}}$ denotes the initial state four-momentum of the parton radiating off the gluon and the transverse momentum of the gluon is given by

$$p_T = \sqrt{sx^2}\frac{z_0}{2}\sin\theta_0\,. \tag{A.18}$$

The $2\to 2$ scattering cross section for $q\bar{q}\to\chi\bar{\chi}$,

$$\sigma_{q\bar{q}\to\chi\bar{\chi}}(s_{23}) = \frac{1}{4}\frac{\overline{|M|^2}_{q\bar{q}\to\chi\bar{\chi}}(s_{23})}{2sx^2(1-z_0)}d\phi_{2,3}^{2\text{body}}\,, \tag{A.19}$$

can be factored out leading to

$$d\sigma_{q\bar{q}\to\chi\bar{\chi}+j(g)} = \sigma_{q\bar{q}\to\chi\bar{\chi}}(s_{23})\frac{\alpha_s}{4\pi}\frac{1+(1-z_0)^2}{z_0}\frac{z_0}{p_T^2}sx^2z_0dz_0d\cos\theta_0 \tag{A.20}$$

$$= \sigma_{q\bar{q}\to\chi\bar{\chi}}(s_{23})\frac{\alpha_s}{\pi}\frac{1+(1-z_0)^2}{z_0}\frac{1}{\sin^2\theta_0}dz_0d\cos\theta_0\,, \tag{A.21}$$

where eq. (A.18) has been used in the last line. Finally the cross section has to expressed in terms of the variables in the lab frame to properly take the detector geometry into account. The change from the so-far considered variables in the centre of mass frame (z_0,θ_0) to the transverse momentum and rapidity of the jet, (p_T,η), leads to the following Jacobian factor

$$\frac{dz_0d\cos\theta_0}{dp_Td\eta} = \frac{4p_T}{sx_1x_2z_0} \tag{A.22}$$

and the old variables can be rewritten as follows

$$\frac{1}{\sin^2\theta_0} = \frac{sx_1x_2}{4p_T^2}z_0^2 \qquad\qquad z_0 = \frac{p_T}{\sqrt{s}}\frac{x_1e^{-\eta}+x_2e^{\eta}}{x_1x_2}\,. \tag{A.23}$$

Finally the color factors have to be included. For gluon emission it is 1/3 for color average, $\text{Tr}[T_aT_a] = 1/2$ and a factor of 8 for the sum over gluons. Thus the color factor is $C_F = 4/3$. The cross section $\sigma_{q\bar{q}\to\chi\bar{\chi}}$ contains the color factor 1/3: $(1/3)^2$ for the color average and

[6] Note that only one of the two diagrams contributes, as only one can be "collinear". Consequently also interference is negligible.

JHEP08(2016)125

3 for the color sum. Thus the color factor for the full 3body cross section is 4/9 and the final expression for the emission of a gluon jet replacing x^2 by $x_1 x_2$ is given by

$$\sigma_{q\bar{q}\to\chi\bar{\chi}+j(g)} = \sum_q \int dx_1 dx_2 dp_T d\eta (f_q(x_1) f_{\bar{q}}(x_2) + f_q(x_2) f_{\bar{q}}(x_1)) \frac{dz d\cos\theta_0}{dp_T d\eta} \sigma_{q\bar{q}\to\chi\bar{\chi}}(s_{23}) P_{q\to g}(z_0, \theta_0) \tag{A.24}$$

with the splitting function

$$P_{q\to g}(z_0, \theta_0) = \frac{4\alpha_s}{3\pi} \frac{1 + (1 - z_0)^2}{z_0 \sin^2\theta_0} \,. \tag{A.25}$$

This expression is consistent with the expression in ref. [37]. The factor 2 for the 2 emissions from the initial quark and anti-quark lines is already taken into account, because the expression is only valid for $\theta \in (0, \theta_{\max})$ for the emission from parton 1 or $\theta \in (\theta_{\max}, \pi)$ for the emission from parton 2. Each time only one of the 2 diagrams contributes. Extending to the maximum, i.e. $\theta_{\max} = \pi/2$, the cross section is given by the calculated expression integrated over the full range of θ, without any additional factor of 2.

Similarly, the cross section for radiating off a quark-jet is given by

$$\sigma_{q\bar{q}\to\chi\bar{\chi}+j(q)} = \sum_q \int dx_1 dx_2 dp_T d\eta \, (f_q(x_1) f_g(x_2) + f_q(x_2) f_g(x_1) + [q \to \bar{q}]) \frac{dz d\cos\theta_0}{dp_T d\eta} \sigma_{q\bar{q}\to\chi\bar{\chi}}(s_{23}) P_{g\to q}(z_0, \theta_0) \,, \tag{A.26}$$

where the splitting function for a quark-jet with n_f different possible quark flavours is

$$P_{g\to q}(z_0, \theta_0) = \frac{n_f \, \alpha_s}{4\pi} \frac{z_0^2 + (1 - z_0)^2}{\sin^2\theta_0} \,. \tag{A.27}$$

B Convention for spinors

We explicitly list the helicity spinors used in our calculations to fix the convention of phases. In the ultra-relativistic limit and setting the azimuthal angle $\phi = 0$, the helicity spinors take the form

$$u_R(E,\theta) = v_L(E,\theta) = \sqrt{2E} \begin{pmatrix} 0 \\ 0 \\ \cos\frac{\theta}{2} \\ i\sin\frac{\theta}{2} \end{pmatrix} \quad u_L(E,\theta) = -v_R(E,\theta) = \sqrt{2E} \begin{pmatrix} i\sin\frac{\theta}{2} \\ \cos\frac{\theta}{2} \\ 0 \\ 0 \end{pmatrix} . \tag{B.1}$$

C K-matrix unitarisation of D5

The T-matrix for $2 \to 2$ scattering of quark - anti-quark and DM-DM two-particle states in case of the effective theory described by the Lagrangian in eq. (4.1) is given by

$$T = -\frac{1}{16\pi^2}\begin{pmatrix} \frac{2s\cos^2\left(\frac{\theta}{2}\right)}{\Lambda_{qq}^2} & 0 & 0 & \frac{s\sin^2\left(\frac{\theta}{2}\right)}{\Lambda_{qq}^2} & \frac{s\cos^2\left(\frac{\theta}{2}\right)}{\Lambda_{q\chi}^2} & 0 & 0 & \frac{s\sin^2\left(\frac{\theta}{2}\right)}{\Lambda_{q\chi}^2} \\ 0 & \frac{s}{\Lambda_{qq}^2} & 0 & 0 & 0 & 0 & 0 & 0 \\ 0 & 0 & \frac{s}{\Lambda_{qq}^2} & 0 & 0 & 0 & 0 & 0 \\ \frac{s\sin^2\left(\frac{\theta}{2}\right)}{\Lambda_{qq}^2} & 0 & 0 & \frac{2s\cos^2\left(\frac{\theta}{2}\right)}{\Lambda_{qq}^2} & \frac{s\sin^2\left(\frac{\theta}{2}\right)}{\Lambda_{q\chi}^2} & 0 & 0 & \frac{s\cos^2\left(\frac{\theta}{2}\right)}{\Lambda_{q\chi}^2} \\ \frac{s\cos^2\left(\frac{\theta}{2}\right)}{\Lambda_{q\chi}^2} & 0 & 0 & \frac{s\sin^2\left(\frac{\theta}{2}\right)}{\Lambda_{q\chi}^2} & \frac{2s\cos^2\left(\frac{\theta}{2}\right)}{\Lambda_{\chi\chi}^2} & 0 & 0 & \frac{s\sin^2\left(\frac{\theta}{2}\right)}{\Lambda_{\chi\chi}^2} \\ 0 & 0 & 0 & 0 & 0 & \frac{s}{\Lambda_{\chi\chi}^2} & 0 & 0 \\ 0 & 0 & 0 & 0 & 0 & 0 & \frac{s}{\Lambda_{\chi\chi}^2} & 0 \\ \frac{s\sin^2\left(\frac{\theta}{2}\right)}{\Lambda_{q\chi}^2} & 0 & 0 & \frac{s\cos^2\left(\frac{\theta}{2}\right)}{\Lambda_{q\chi}^2} & \frac{s\sin^2\left(\frac{\theta}{2}\right)}{\Lambda_{\chi\chi}^2} & 0 & 0 & \frac{2s\cos^2\left(\frac{\theta}{2}\right)}{\Lambda_{\chi\chi}^2} \end{pmatrix} \tag{C.1}$$

in the basis $(|q_L\bar{q}_R\rangle, |q_L\bar{q}_L\rangle, |q_R\bar{q}_R\rangle, |q_R\bar{q}_L\rangle, |\chi_L\bar{\chi}_R\rangle, |\chi_L\bar{\chi}_L\rangle, |\chi_R\bar{\chi}_R\rangle, |\chi_R\bar{\chi}_L\rangle)$. The two-particle states with the same helicity, completely decouple from the other states and can be treated separately. They are pairwise related by parity and they only contribute to the $J = 0$ term in the partial wave expansion

$$\langle q_L\bar{q}_L|T^0|q_L\bar{q}_L\rangle = \langle q_R\bar{q}_R|T^0|q_R\bar{q}_R\rangle = -\frac{1}{4\pi}\frac{s}{\Lambda_{qq}^2} \tag{C.2}$$

$$\langle \chi_L\bar{\chi}_L|T^0|\chi_L\bar{\chi}_L\rangle = \langle \chi_R\bar{\chi}_R|T^0|\chi_R\bar{\chi}_R\rangle = -\frac{1}{4\pi}\frac{s}{\Lambda_{\chi\chi}^2}\,. \tag{C.3}$$

Thus the only non-vanishing elements of the unitarised T-matrix, T^0, are given by

$$\langle q_L\bar{q}_L|T_U^0|q_L\bar{q}_L\rangle = \langle q_R\bar{q}_R|T_U^0|q_R\bar{q}_R\rangle = \frac{is}{s - 4\pi i\Lambda_{qq}^2} \tag{C.4}$$

$$\langle \chi_L\bar{\chi}_L|T_U^0|\chi_L\bar{\chi}_L\rangle = \langle \chi_R\bar{\chi}_R|T_U^0|\chi_R\bar{\chi}_R\rangle = \frac{is}{s - 4\pi i\Lambda_{\chi\chi}^2}\,. \tag{C.5}$$

The remaining states with opposite helicities contribute to the $J = 1$ term in the partial wave expansion. The 4×4 sub-block of the T-matrix, T^1, in the basis $(|q_L\bar{q}_R\rangle, |q_R\bar{q}_L\rangle, |\chi_L\bar{\chi}_R\rangle, |\chi_R\bar{\chi}_L\rangle)$ is given by

$$T^1 = -\frac{1}{12\pi}\begin{pmatrix} \frac{2s}{\Lambda_{qq}^2} & \frac{s}{\Lambda_{qq}^2} & \frac{s}{\Lambda_{q\chi}^2} & \frac{s}{\Lambda_{q\chi}^2} \\ \frac{s}{\Lambda_{qq}^2} & \frac{2s}{\Lambda_{qq}^2} & \frac{s}{\Lambda_{q\chi}^2} & \frac{s}{\Lambda_{q\chi}^2} \\ \frac{s}{\Lambda_{q\chi}^2} & \frac{s}{\Lambda_{q\chi}^2} & \frac{2s}{\Lambda_{\chi\chi}^2} & \frac{s}{\Lambda_{\chi\chi}^2} \\ \frac{s}{\Lambda_{q\chi}^2} & \frac{s}{\Lambda_{q\chi}^2} & \frac{s}{\Lambda_{\chi\chi}^2} & \frac{2s}{\Lambda_{\chi\chi}^2} \end{pmatrix}\,. \tag{C.6}$$

Many of the elements are related by the time-reversal symmetry and parity. [28, 41] There are only 6 independent matrix elements and we find for the independent elements of the

JHEP08(2016)125

unitarised T-matrix T_U^1

$$\langle q_L\bar{q}_R|T_U^1|q_L\bar{q}_R\rangle = \frac{s\left(48\pi\Lambda_{q\chi}^2 r^4 s + ir^2\left(5s^2-288\pi^2\Lambda_{q\chi}^4\right)+36\pi\Lambda_{q\chi}^2 s\right)}{\left(s-12i\pi\Lambda_{q\chi}^2 r^2\right)\left(-36i\pi\Lambda_{q\chi}^2 r^4 s + r^2\left(5s^2-144\pi^2\Lambda_{q\chi}^4\right)-36i\pi\Lambda_{q\chi}^2 s\right)} \tag{C.7}$$

$$\langle q_L\bar{q}_R|T_U^1|q_R\bar{q}_L\rangle = \frac{12\pi\Lambda_{q\chi}^2 r^2 s\left(r^2 s-12i\pi\Lambda_{q\chi}^2\right)}{\left(s-12i\pi\Lambda_{q\chi}^2 r^2\right)\left(-36i\pi\Lambda_{q\chi}^2 r^4 s + r^2\left(5s^2-144\pi^2\Lambda_{q\chi}^4\right)-36i\pi\Lambda_{q\chi}^2 s\right)} \tag{C.8}$$

$$\langle q_L\bar{q}_R|T_U^1|\chi_L\bar{\chi}_R\rangle = -\frac{12\pi\Lambda_{q\chi}^2 r^2 s}{36i\pi\Lambda_{q\chi}^2 r^4 s + r^2\left(144\pi^2\Lambda_{q\chi}^4-5s^2\right)+36i\pi\Lambda_{q\chi}^2 s} \tag{C.9}$$

$$\langle q_L\bar{q}_R|T_U^1|\chi_R\bar{\chi}_L\rangle = \langle q_L\bar{q}_R|T_U^1|\chi_L\bar{\chi}_R\rangle \tag{C.10}$$

$$\langle \chi_L\bar{\chi}_R|T_U^1|\chi_L\bar{\chi}_R\rangle = \langle q_L\bar{q}_R|T_U^1|q_L\bar{q}_R\rangle\left[r\to\frac{1}{r}\right] \tag{C.11}$$

$$\langle \chi_L\bar{\chi}_R|T_U^1|\chi_R\bar{\chi}_L\rangle = \langle q_L\bar{q}_R|T_U^1|q_R\bar{q}_L\rangle\left[r\to\frac{1}{r}\right]. \tag{C.12}$$

The fourth equation follows from the interaction being vector-like and the last two equations follow from the symmetry $q \leftrightarrow \chi$. The remaining matrix elements can be obtained from time-reversal and parity symmetry: time reversal symmetry implies that T_U^1 is symmetric, i.e. $T_U^1 = \left(T_U^1\right)^T$. Parity conservation implies that matrix elements are invariant under flipping all helicities, i.e. $\langle\lambda_1'\lambda_2'|T_U^1|\lambda_1\lambda_2\rangle = \langle -\lambda_1' - \lambda_2'|T_U^1|-\lambda_1-\lambda_2\rangle$.

D Effective SM-WIMP operators

We list the operators coupling the SM to Dirac fermion WIMPs [7] in table 1.

Name	D1	D2	D3	D4	D5
Op.	$\bar{\chi}\chi\bar{q}q$	$\bar{\chi}\gamma^5\chi\bar{q}q$	$\bar{\chi}\chi\bar{q}\gamma^5 q$	$\bar{\chi}\gamma^5\chi\bar{q}\gamma^5 q$	$\bar{\chi}\gamma^\mu\chi\bar{q}\gamma_\mu q$
Name	D6	D7	D8	D9	D10
Op	$\bar{\chi}\gamma^\mu\gamma^5\chi\bar{q}\gamma_\mu q$	$\bar{\chi}\gamma^\mu\chi\bar{q}\gamma_\mu\gamma^5 q$	$\bar{\chi}\gamma^\mu\gamma^5\chi\bar{q}\gamma_\mu\gamma^5 q$	$\bar{\chi}\sigma^{\mu\nu}\chi\bar{q}\sigma_{\mu\nu}q$	$\bar{\chi}\sigma_{\mu\nu}\gamma^5\chi\bar{q}\sigma_{\alpha\beta}q$
Name	D11	D12	D13	D14	
Op	$\bar{\chi}\chi G_{\mu\nu}G^{\mu\nu}$	$\bar{\chi}\gamma^5\chi G_{\mu\nu}G^{\mu\nu}$	$\bar{\chi}\chi G_{\mu\nu}\tilde{G}^{\mu\nu}$	$\bar{\chi}\gamma^5\chi G_{\mu\nu}\tilde{G}^{\mu\nu}$	

Table 1. Operators coupling SM to WIMPs first shown in ref. [7].

References

[1] ATLAS collaboration, *Search for dark matter candidates and large extra dimensions in events with a jet and missing transverse momentum with the ATLAS detector*, *JHEP* **04** (2013) 075 [arXiv:1210.4491] [INSPIRE].

JHEP08(2016)125

[2] CMS collaboration, *Search for New Physics with a Mono-Jet and Missing Transverse Energy in pp Collisions at $\sqrt{s} = 7$ TeV*, *Phys. Rev. Lett.* **107** (2011) 201804 [arXiv:1106.4775] [INSPIRE].

[3] ATLAS collaboration, *Search for new phenomena in final states with an energetic jet and large missing transverse momentum in pp collisions at $\sqrt{s} = 8$ TeV with the ATLAS detector*, *Eur. Phys. J.* **C 75** (2015) 299 [arXiv:1502.01518] [INSPIRE].

[4] CMS collaboration, *Search for dark matter, extra dimensions and unparticles in monojet events in proton-proton collisions at $\sqrt{s} = 8$ TeV*, *Eur. Phys. J.* **C 75** (2015) 235 [arXiv:1408.3583] [INSPIRE].

[5] ATLAS collaboration, *Search for new phenomena in final states with an energetic jet and large missing transverse momentum in pp collisions at $\sqrt{s} = 13$ TeV using the ATLAS detector*, arXiv:1604.07773 [INSPIRE].

[6] CMS collaboration, *Search for dark matter with jets and missing transverse energy at 13 TeV*, CMS-PAS-EXO-15-003 (2015).

[7] J. Goodman, M. Ibe, A. Rajaraman, W. Shepherd, T.M.P. Tait and H.-B. Yu, *Constraints on Dark Matter from Colliders*, *Phys. Rev.* **D 82** (2010) 116010 [arXiv:1008.1783] [INSPIRE].

[8] J. Goodman, M. Ibe, A. Rajaraman, W. Shepherd, T.M.P. Tait and H.-B. Yu, *Constraints on Light Majorana dark Matter from Colliders*, *Phys. Lett.* **B 695** (2011) 185 [arXiv:1005.1286] [INSPIRE].

[9] M. Endo and Y. Yamamoto, *Unitarity Bounds on Dark Matter Effective Interactions at LHC*, *JHEP* **06** (2014) 126 [arXiv:1403.6610] [INSPIRE].

[10] I.M. Shoemaker and L. Vecchi, *Unitarity and Monojet Bounds on Models for DAMA, CoGeNT and CRESST-II*, *Phys. Rev.* **D 86** (2012) 015023 [arXiv:1112.5457] [INSPIRE].

[11] S. El Hedri, W. Shepherd and D.G.E. Walker, *Perturbative Unitarity Constraints on Gauge Portals*, arXiv:1412.5660 [INSPIRE].

[12] Y. Yamamoto, *Unitarity bounds on scalar dark matter effective interactions at LHC*, *PTEP* **2014** (2014) 123B03 [arXiv:1409.5775] [INSPIRE].

[13] D. Abercrombie et al., *Dark Matter Benchmark Models for Early LHC Run-2 Searches: Report of the ATLAS/CMS Dark Matter Forum*, arXiv:1507.00966 [INSPIRE].

[14] N.F. Bell, Y. Cai, J.B. Dent, R.K. Leane and T.J. Weiler, *Dark matter at the LHC: Effective field theories and gauge invariance*, *Phys. Rev.* **D 92** (2015) 053008 [arXiv:1503.07874] [INSPIRE].

[15] N.F. Bell, Y. Cai and R.K. Leane, *Mono-W Dark Matter Signals at the LHC: Simplified Model Analysis*, *JCAP* **01** (2016) 051 [arXiv:1512.00476] [INSPIRE].

[16] U. Haisch, F. Kahlhoefer and T.M.P. Tait, *On Mono-W Signatures in Spin-1 Simplified Models*, *Phys. Lett.* **B 760** (2016) 207 [arXiv:1603.01267] [INSPIRE].

[17] C. Englert, M. McCullough and M. Spannowsky, *S-Channel Dark Matter Simplified Models and Unitarity*, arXiv:1604.07975 [INSPIRE].

[18] F. Kahlhoefer, K. Schmidt-Hoberg, T. Schwetz and S. Vogl, *Implications of unitarity and gauge invariance for simplified dark matter models*, *JHEP* **02** (2016) 016 [arXiv:1510.02110] [INSPIRE].

[19] N.F. Bell, Y. Cai and R.K. Leane, *Dark Forces in the Sky: Signals from Z' and the Dark Higgs*, *JCAP* **08** (2016) 001 [arXiv:1605.09382] [INSPIRE].

JHEP08(2016)125

[20] G. Busoni, A. De Simone, E. Morgante and A. Riotto, *On the Validity of the Effective Field Theory for Dark Matter Searches at the LHC*, *Phys. Lett.* **B 728** (2014) 412 [arXiv:1307.2253] [INSPIRE].

[21] G. Busoni, A. De Simone, J. Gramling, E. Morgante and A. Riotto, *On the Validity of the Effective Field Theory for Dark Matter Searches at the LHC, Part II: Complete Analysis for the s-channel*, *JCAP* **06** (2014) 060 [arXiv:1402.1275] [INSPIRE].

[22] G. Busoni, A. De Simone, T. Jacques, E. Morgante and A. Riotto, *On the Validity of the Effective Field Theory for Dark Matter Searches at the LHC Part III: Analysis for the t-channel*, *JCAP* **09** (2014) 022 [arXiv:1405.3101] [INSPIRE].

[23] E.P. Wigner, *Resonance Reactions and Anomalous Scattering*, *Phys. Rev.* **70** (1946) 15 [INSPIRE].

[24] E.P. Wigner and L. Eisenbud, *Higher Angular Momenta and Long Range Interaction in Resonance Reactions*, *Phys. Rev.* **72** (1947) 29 [INSPIRE].

[25] S.U. Chung et al., *Partial wave analysis in K matrix formalism*, *Annalen Phys.* **4** (1995) 404.

[26] S.U. Chung, *Spin formalisms*, third updated version of CERN-71-08.

[27] M. Jacob and G.C. Wick, *On the general theory of collisions for particles with spin*, *Annals Phys.* **7** (1959) 404 [INSPIRE].

[28] A.D. Martin and T.D. Spearman, *Elementary Particle Theory*, North-Holland/Wiley, Amsterdam/New York (1970).

[29] W. Kilian, T. Ohl, J. Reuter and M. Sekulla, *High-Energy Vector Boson Scattering after the Higgs Discovery*, *Phys. Rev.* **D 91** (2015) 096007 [arXiv:1408.6207] [INSPIRE].

[30] T.N. Truong, *Remarks on the unitarization methods*, *Phys. Rev. Lett.* **67** (1991) 2260 [INSPIRE].

[31] S.N. Gupta, *Theory of longitudinal photons in quantum electrodynamics*, *Proc. Phys. Soc.* **A 63** (1950) 681 [INSPIRE].

[32] S.N. Gupta, *Quantum Electrodynamics*, Gordon and Breach (1977).

[33] W. Heitler, *The influence of radiation damping on the scattering of light and mesons by free particles. I*, *Math. Proc. Camb. Phil. Soc.* **37** (1941) 291.

[34] J.S. Schwinger, *Quantum electrodynamics. I. A covariant formulation*, *Phys. Rev.* **74** (1948) 1439 [INSPIRE].

[35] A. Alboteanu, W. Kilian and J. Reuter, *Resonances and Unitarity in Weak Boson Scattering at the LHC*, *JHEP* **11** (2008) 010 [arXiv:0806.4145] [INSPIRE].

[36] R.L. Delgado, A. Dobado and F.J. Llanes-Estrada, *Unitarity, analyticity, dispersion relations and resonances in strongly interacting W_LW_L, Z_LZ_L and hh scattering*, *Phys. Rev.* **D 91** (2015) 075017 [arXiv:1502.04841] [INSPIRE].

[37] A. Birkedal, K. Matchev and M. Perelstein, *Dark matter at colliders: A model independent approach*, *Phys. Rev.* **D 70** (2004) 077701 [hep-ph/0403004] [INSPIRE].

[38] ATLAS collaboration, *Sensitivity to WIMP Dark Matter in the Final States Containing Jets and Missing Transverse Momentum with the ATLAS Detector at 14 TeV LHC*, ATL-PHYS-PUB-2014-007 (2014).

JHEP08(2016)125

[39] ATLAS collaboration, *Search for new phenomena in dijet mass and angular distributions from pp collisions at* $\sqrt{s} = 13$ *TeV with the ATLAS detector*, *Phys. Lett.* **B 754** (2016) 302 [arXiv:1512.01530] [INSPIRE].

[40] M.E. Peskin and D.V. Schroeder, *An Introduction to quantum field theory*, Addison-Wesley, Reading, U.S.A. (1995).

[41] M.L. Goldberger, M.T. Grisaru, S.W. MacDowell and D.Y. Wong, *Theory of low-energy nucleon-nucleon scattering*, *Phys. Rev.* **120** (1960) 2250 [INSPIRE].

JHEP08(2016)125